Transient solvent dynamics and incoherent control of photodissociation pathways in I_2^- cluster ions

Andrei Sanov, Sreela Nandi, and W. Carl Lineberger
JILA and Department of Chemistry and Biochemistry, University of Colorado, Boulder, Colorado 80309-0440

(Received 7 January 1998; accepted 23 January 1998)

Detailed time-resolved photodissociation and caging dynamics in clusters are studied using $I_2^-(OCS)_{11}$ as a model system. We report new observations of product channel-dependent properties of nuclear coherence in the dissociated chromophore, reflecting complex dynamics of the solvent cage. The coherence feature is most pronounced in the caged two-photon channels and its relative amplitude increases with the product size. Shorter delays, on the time scale of coherent $I\cdots I^-$ motion, favor larger products, allowing for incoherent control of two-photon dissociation pathways by appropriately timing the two laser pulses. As an example of such control, $I_2^-(OCS)_2$ is produced most effectively by a limited set of pump–probe excitations at short delays. We emphasize generality of these results that relate to caging dynamics in any cluster ions. © *1998 American Institute of Physics.* [S0021-9606(98)03513-2]

Clusters offer a potentially well-characterized environment[1–4] for the study of chemical reactions, including solvent-induced recombination, or ''caging'' of photofragments.[5–15] Many groups have investigated caging in real time by monitoring the recovery of the dissociated chromophore's ability to absorb light,[16–26] or following the evolution of the photoelectron spectrum.[27–29] We have emphasized the dynamics of dihalogen anion recombination in size-selected cluster ions.[30–37] The gas-phase environment allows not only selecting the initial solvation conditions,[3] but also probing the disintegrating cluster by a second photon, mass-analyzing the two-photon products to get a glimpse of the evolving cluster structure following photodissociation of the chromophore within the cluster.[30,32]

Our previous studies of photodissociation dynamics[30–32,34–36] generally summed the probe absorption signal over all product masses; only in this fashion was sufficient signal-to-noise ratio achieved to obtain detailed absorption recovery curves. The action signal in individual product channels gave hints of different behaviors for different ionic products, but the combination of product mass resolution, good time resolution and high quality signal statistics was not possible. In this work, we present recombination action spectra for distinct two-photon dissociation pathways obtained using our improved cluster ion apparatus and more elaborate data collection algorithm.

These channel-resolved action spectra allow examination of the caging dynamics in unprecedented detail. The data show that coherent motion of the chromophore cannot be considered separately from dynamics of the cage, and that the evolving solvent configuration favors different types of two-photon products at various stages of evolution. While we employed $I_2^-(OCS)_{11}$ in this study, the results reflect the general dynamics of caging and will be applicable to other solvated systems, e.g., $I_2^-(CO_2)_{16}$.[38]

One important finding in the studies of caging has been the observation of coherent motion of the chromophore persisting for several picoseconds following photodissociation.[19,22,30,31,34] Laser-induced nuclear coherence has been extensively studied in bound-bound molecular transitions[39,40] and successfully applied to exert coherent control of chemical reaction pathways.[41–45] Coherent motion following excitation to a dissociative potential is fundamentally different, since the long-range forces that reverse the motion of photofragments arise entirely from interaction with surrounding solvent.[13,19,22,30]

In I_2^- based clusters, solvent-induced coherent $I\cdots I^-$ motion is manifest as an early delay-time ''bump'' in transient absorption data.[30,31,34] The preponderance of available evidence indicates that the maximum of this feature at about 2 ps corresponds to wave packet localization in a Franck–Condon region on either the slightly bound first excited $^2\Pi_{g,3/2}$ or the ground $^2\Sigma^+_{u,1/2}$ electronic state potential[46,47] of I_2^-, or both.[30] The assignment of the state(s) responsible for the coherence feature is extremely difficult because of the substantial solvent-induced perturbations of the I_2^- potentials at large interatomic distances.[46,48]

The product-channel-resolved action spectra presented here show that the time dependence of the absorption recovery is both very complex and strongly dependent upon the two-photon product channel selected for monitoring. The 2 ps coherence peak is most prominent in the highest mass *caged* product channels, making only a minor appearance in the *uncaged* two-photon product channels. The evolving mass distribution also affords an opportunity to employ a specific pump–probe sequence to produce two photon products that are absent at both long and short delay times. This result constitutes a form of incoherent control of recombination pathways in a 35-atom system.

As a detailed description of the ion beam apparatus has been given elsewhere,[49] we emphasize here only those aspects important to the success of the present experiment. In

brief, the ion machine consists of a cluster ion source and a tandem time-of-flight (TOF) mass spectrometer. The $I_2^-(OCS)_n$ clusters are formed by attachment of slow secondary electrons to neutral species in an electron-impact ionized free jet (80 Hz) with subsequent solvent nucleation around the negatively charged core. Initial cluster ion mass selection is achieved in a Wiley–McLaren TOF mass spectrometer, while mass analysis of the ionic fragments is carried out utilizing a second, reflection, mass spectrometer. The reflected fragments are counted with a three-plate microchannel detector. As many as four different mass photofragment ions can be collected simultaneously. The two-photon products are lighter than one-photon products and the one- and two-photon fragment mass distributions do not overlap. The precursor ion signal is monitored with another analog microchannel plate detector positioned directly behind the reflectron; this signal is utilized to normalize the pump–probe product signal to the parent ion intensity.

The femtosecond laser[33] delivers 790 nm, 120 fs pump and probe pulses with a 400 Hz repetition rate. The copropagating pump and probe beams (250 μJ/pulse each) have parallel polarizations and are mildly focused to an ~3 mm diameter spot size in the interaction region. Background subtraction is performed with the use of computer-controlled shutters in the pump and probe beam paths. To better average out fluctuations, the data acquisition algorithm[30] was modified to include a rapid repetition of identical short experimental cycles including several preset delay times interlaced with background acquisitions.[38]

The bare I_2^- ion has bond strength of ~1 eV, and exhibits a dissociative continuum absorption peaking near 790 nm, giving a ~0.5 eV kinetic energy release to the photoproducts.[29,47] One-photon dissociation of I_2^- within a cluster generally leads to both caged and uncaged ionic products.[36,50] In 790 nm dissociation of $I_2^-(OCS)_{11}$, 80% of the one-photon fragments are caged, with the most abundant products[50] being $I_2^-(OCS)_4$ and $I_2^-(OCS)_5$. Subsequent fragmentation of these caged products with a second, probe photon (at long delay allowing complete relaxation of one-photon fragments) yields about 80% uncaged $[I^-(OCS)_{2,3,4}]$ and 20% caged $[I_2^-(OCS)_{0,1}]$ products.

The two-photon dissociation experiments at long delays are only sensitive to those one-photon trajectories that have led to the recombinations of the chromophore, as only caged one-photon fragments can absorb a second 790 nm photon. However, at earlier times (less than ~5 ps) the distinction between one-photon trajectories ultimately leading to caged and uncaged products is ambiguous, and even clusters *en route* to uncaged fragments can conceivably absorb a probe photon.

The top curve in Fig. 1(a) depicts the photoabsorption recovery signal for $I_2^-(OCS)_{11}$, obtained by combining all major two-photon products. The curve exhibits a coherence maximum at about 2.5 ps. As in the earlier studies with CO_2 solvent,[30] the bump corresponds to the dissociated chromophore, arrested by the solvent shell, returning to the Franck–Condon region. The absorption decrease just after 2.5 ps corresponds to the subsequent departure of the chromophore from the Franck–Condon region and the further

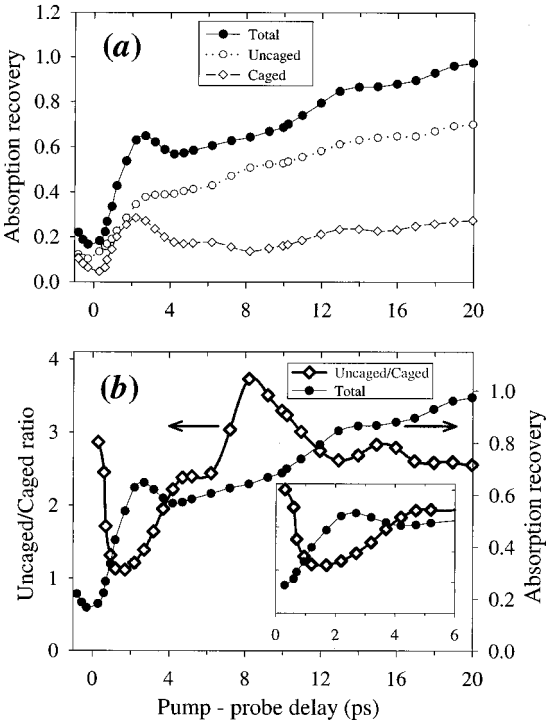

FIG. 1. (a) Total absorption recovery signal obtained by combining all major two-photon products in the photodissociation of $I_2^-(OCS)_{11}$ at 790 nm and the ''caged'' and ''uncaged'' components obtained by counting the respective types of two-photon products separately. (b) Delay-dependence of the uncaged/caged ratio, compared to the total absorption recovery curve reproduced from (a).

absorption recovery represents vibrational relaxation of the recombined chromophore and evaporation of solvent from the cluster. Just as with CO_2 solvent,[30] this bump indicates that a photoexcited ensemble of $\sim 10^7$ clusters undergoes coherent motion of the chromophore for a period of the order of several picoseconds following photodissociation. The 2.5 ps time for the recurrence is much slower than the bound I_2^- vibrational period because it reflects the dissociating chromophore being arrested by the solvent cage and subsequently being returned to the Franck–Condon region. Accordingly, this time is better regarded as a ''solvent'' time, rather than a ''chromophore'' time. The 2.5 ps recurrence time with the OCS solvent is longer than the 1.4 ps time observed for CO_2 solvent.[30,38] The bump in the absorption recovery reveals nothing about any possible coherent motion on the part of the solvent itself.

It is possible, however, to decompose this total absorption recovery curve in such a way as to provide direct information about possible coherent motion of the solvent itself. This can be accomplished by following the absorption recovery as detected by specific two-photon products, as these products reflect the structure of the solvent cage at a given delay time. By determining the mass of each of the two-photon ionic photoproducts, the absorption recovery curve can be decomposed into ''caged'' and ''uncaged'' components, as shown in Fig. 1(a). These two components arise from different instantaneous solvent configurations. It is immediately clear that the coherence feature in the total absorption recovery arises primarily from the caged two-photon

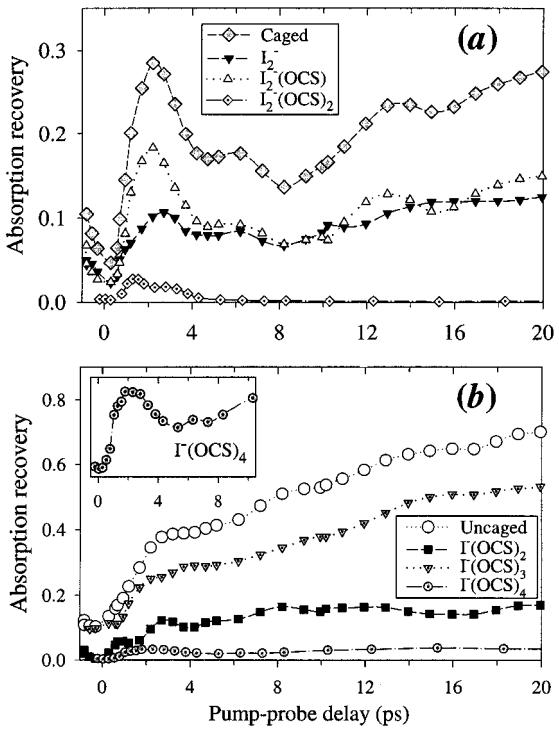

FIG. 2. (a) Caged component of the absorption recovery [reproduced from Fig. 1(a)] and contributions of individual caged two-photon channels. (b) Same for the uncaged two-photon channels. Inset shows a blow-up of the coherence feature in the $I^-(OCS)_4$ channel.

pathways. The caged component exhibits complicated time-dependent dynamics, while the uncaged component essentially grows monotonically, exhibiting only a shoulder around the time of the coherence peak.

Further understanding of the dynamics can be gained by examining the ratio of the uncaged and caged components as a function of probe delay, as shown in Fig. 1(b). The ratio measurement has the enormous advantage that it is independent of the fraction of the initially excited ions that have recombined, and evolution of this ratio as a function of delay directly reflect changes in the solvent configuration. In the statistical, incoherent limit, we would expect this ratio to increase monotonically to the observed long delay uncaged/caged ratio, $\sim$3. In fact, a very different behavior is observed. Rather, this ratio decreases to a minimum at about 1.8 ps and then increases to reach a maximum at $\sim$8 ps. As the delay time increases, this ratio levels off at the statistical asymptote.

Further reducing the level of channel averaging, Fig. 2 shows the behavior of specific caged [Fig. 2(a)] and uncaged [Fig. 2(b)] two-photon photoproducts. The relative amplitude of the coherence feature depends not only on the caged or uncaged nature of the final product, but also on the number of remaining solvent molecules, increasing with the product size. The most pronounced effect is in the $I_2^-(OCS)_2$ channel; its yield is almost unobservable at long delays ($<$0.4%), however, substantial dissociation occurs in a narrow delay window coinciding with the characteristic time-scale of $I\cdots I^-$ coherent motion. As another example, no noticeable coherence peak is revealed in the major uncaged channels; only the heaviest (and minor) uncaged product, $I^-(OCS)_4$, exhibits a clear early-time bump, as seen in the inset in Fig. 2(b). We also note that the maximum of the coherence feature in $I_2^-(OCS)_2$ is shifted to about 40% shorter delay compared to I_2^- and $I_2^-(OCS)$.

To summarize the experimental observations, the coherence-induced recurrences are complex, nonstatistical and product channel-dependent. (i) The coherence feature derives mainly from those dissociation trajectories that terminate in caged two-photon products. (ii) The two-photon uncaged/caged branching ratio exhibits nonstatistical time-evolution, having a minimum at $<$2 ps, peaking after the coherence feature and leveling off at the statistical asymptote at $>$12 ps. (iii) The relative amplitude of the coherence feature increases with the caged two-photon product mass. (iv) The heaviest caged two-photon fragment $I_2^-(OCS)_2$, contributes to the earlier portion of the coherence peak, while the lighter $I_2^-(OCS)$ and I_2^- fragments are the major components of the later part of the peak.

While the coherence peak is much stronger in the caged two-photon channels, the pump–probe signals in the major uncaged channels better correspond to statistical expectations, reflecting the gradual relaxation of I_2^-. This difference stems from the solvent cage favoring either the caged or uncaged two-photon products at different stages of its evolution. Following absorption of the first photon, solute–solvent interactions are likely to excite a ''breathing'' mode of the cage (which is certainly *not* a normal mode, since even the number of solvent molecules is not conserved in time). The dynamics following the absorption of the second photon will be strongly affected by the phase of the solvent cage ''breathing mode'' at the time of the second photon absorption. Caging following the second photon absorption is likely enhanced by the solvent cage moving inward, while the uncaged products would be favored when the cage is expanding. This is what we believe to be observed around the minimum in the caging ratio at $\sim$2 ps. These oscillations in the uncaged/caged branching ratio would rapidly be damped by loss of solvent coherence, and the ratio will revert to statistical behavior.

The number of solvent molecules lost by the cluster in this sequential two-photon process is decreased if the second photon arrives at a time that favors unusually large kinetic release to a solvent molecule. The effectiveness of the energy transfer from photoexcited I_2^- to individual solvent molecules is dependent on the relative phase of the I_2^- and cage motion. The best time for large energy transfer is the same as for enhanced caging: when $I\cdots I^-$ and the solvent cage are out of phase with each other, with the cage moving inwards. Therefore, larger two-photon products are favored at the same delays as when the uncaged/caged ratio is at its minimum, just before the coherence peak in transient absorption. Additionally, in this short delay window, the energy of both photons is effectively combined in a single ($I\cdots I^-$) degree of freedom, thus favoring impulsive interaction with the solvent. These factors enhance the coherence feature in *larger* caged two-photon channels.

An extreme example of this effect is the production of $I_2^-(OCS)_2$ predominantly with pump–probe separations of

~1 to 4 ps, sharply peaking at 1.4 ps. This result demonstrates a method to control two-photon dissociation pathways by appropriately timing the two laser pulses. We emphasize the *incoherent* nature of this effect, in contrast to the coherent wave packet methods of reaction control.[41,43,44,51] The rapid decrease int he $I_2^-(OCS)_2$ yield at 4 ps reflects the solvent dynamics rather than the $I\cdots I^-$ coherence. Other incoherent methods of control are based on the use of interference,[42,52] femtosecond ponderomotive forces,[53] and the feedback control.[54] This control and the ratio measurement in Fig. 1(b) indicates that coherence and non-statistical behavior can persist for at least ~8 ps in a 35-atom complex.

The maximum $I_2^-(OCS)_2$ occurs at the time of the minimum of the uncaged/caged ratio, rather than at the time of the transient absorption coherence peak. This result is a clear indication that, for the production of this ''abnormally large'' fragment, the optimal localization of the $I\cdots I^-$ wave packet in the Franck–Condon region is not the most important prerequisite. The determining factor for this channel is a large (impulsive) translational energy release which is only possible at short delays, near the bottom of the uncaged/caged curve well [see Fig. 1(b)].

In conclusion, we have shown that I_2^- dissociation and recombination dynamics within an evolving cluster are very complex, nonstatistical and dependent on the composition of the monitored two-photon products. The coherence feature is most pronounced in the caged two-photon channels and its relative amplitude increases with the product size. Time-dependence of the two-photon uncaged/caged branching ratio reflects the dynamics of the solvent cage. Observation of a transient product channel in the dissociation of $I_2^-(OCS)_{11}$ demonstrates incoherent control of two-photon dissociation pathways by appropriately timing the two laser pulses.

Although the results presented here are for a single cluster ion, the main conclusions are general and pertain to gas-phase caging dynamics in any cluster ions. For example, similar results were obtained for $I_2^-(CO_2)_{16}$.[38]

The authors acknowledge the helpful assistance of Dr. Doo Wan Boo. This research is funded by the National Science Foundation (Grant Nos. CHE97-03486 and PHY95-12150) and the Air Force Office of Scientific Research (AASERT program).

[1] A. W. Castleman and K. H. Bowen, J. Phys. Chem. **100**, 12911 (1996).
[2] J. M. Farrar, in *Current Topics in Ion Chemistry and Physics*, edited by C. Y. Ng and I. Powis (Wiley, New York, 1992).
[3] M. A. Johnson and W. C. Lineberger, in *Techniques for the Study of Ion Molecule Reactions*, edited by J. M. Farrar and J. W. Saunders (Wiley, New York, 1988), p. 591.
[4] A. W. Castleman, Jr., in *Clusters of Atoms and Molecules*, edited by H. Haberland (Springer-Verlag, New York, 1992).
[5] J. Troe, Annu. Rev. Phys. Chem. **29**, 223 (1978).
[6] B. Otto, J. Schroeder, and J. Troe, J. Chem. Phys. **81**, 202 (1984).
[7] H. Kunz, J. G. McCaffrey, R. Schriever, and N. Schwentner, J. Chem. Phys. **94**, 1039 (1991).
[8] J. Xu, N. Schwentner, and M. Chergui, J. Chem. Phys. **101**, 7381 (1994).
[9] K. H. Godderz, N. Schwentner, and M. Chergui, J. Chem. Phys. **105**, 451 (1996).
[10] V. E. Bondybey and L. E. Brus, Adv. Chem. Phys. **41**, 269 (1980).
[11] P. S. Dardi and J. S. Dahler, J. Chem. Phys. **93**, 242 (1990).
[12] G. N. R. Tripathi, R. H. Schuler, and R. W. Fessenden, Chem. Phys. Lett. **113**, 563 (1985).
[13] V. S. Batista and D. F. Coker, J. Chem. Phys. **106**, 7102 (1997).
[14] B. M. Ladanyi and R. Parson, J. Chem. Phys. **107**, 9326 (1997).
[15] N. Delaney, J. Faeder, P. E. Maslen, and R. Parson, J. Phys. Chem. A **101**, 8147 (1997).
[16] X. Xu, S. Yu, R. Lingle, H. Zhu, and J. B. Hopkins, J. Chem. Phys. **95**, 2445 (1991).
[17] A. L. Harris, J. K. Brown, and C. B. Harris, Annu. Rev. Phys. Chem. **39**, 341 (1988).
[18] R. Zadoyan, Z. Li, C. C. Martens, and V. A. Apkarian, J. Chem. Phys. **101**, 6648 (1994).
[19] R. Zadoyan, Z. Li, P. Ashjian, C. C. Martens, and V. A. Apkarian, Chem. Phys. Lett. **218**, 504 (1994).
[20] Q. Liu, J. K. Wang, and A. H. Zewail, Nature (London) **364**, 427 (1993).
[21] E. D. Potter, Q. Liu, and A. H. Zewail, Chem. Phys. Lett. **200**, 605 (1992).
[22] Q. L. Liu, J. K. Wang, and A. H. Zewail, J. Phys. Chem. **99**, 11321 (1995).
[23] J. K. Wang, Q. L. Liu, and A. H. Zewail, J. Phys. Chem. **99**, 11309 (1995).
[24] A. E. Johnson, N. E. Levinger, and P. F. Barbara, J. Phys. Chem. **96**, 7841 (1992).
[25] D. A. V. Kliner, J. C. Alfano, and P. F. Barbara, J. Chem. Phys. **98**, 5375 (1993).
[26] J. C. Alfano, Y. Kimura, P. K. Walhout, and P. F. Barbara, Chem. Phys. **175**, 147 (1993).
[27] B. J. Greenblatt, M. T. Zanni, and D. M. Neumark, Science **276**, 1675 (1997).
[28] R. Parson and J. Faeder, Science **276**, 1660 (1997).
[29] B. J. Greenblatt, M. T. Zanni, and D. M. Neumark, Chem. Phys. Lett. **258**, 523 (1996).
[30] J. M. Papanikolas, V. Vorsa, M. E. Nadal, P. J. Campagnola, H. K. Buchenau, and W. C. Lineberger, J. Chem. Phys. **99**, 8733 (1993).
[31] J. M. Papanikolas, V. Vorsa, M. E. Nadal, P. J. Campagnola, J. R. Gord, and W. C. Lineberger, J. Chem. Phys. **97**, 7002 (1992).
[32] V. Vorsa, S. Nandi, P. J. Campagnola, M. Larsson, and W. C. Lineberger, J. Chem. Phys. **106**, 1402 (1997).
[33] V. Vorsa, P. J. Campagnola, S. Nandi, M. Larsson, and W. C. Lineberger, J. Chem. Phys. **105**, 2298 (1996).
[34] M. E. Nadal, S. Nandi, D. W. Boo, and W. C. Lineberger, J. Chem. Phys. (to be published).
[35] J. M. Papanikolas, P. J. Campagnola, V. Vorsa, M. E. Nadal, H. K. Buchenau, R. Parson, and W. C. Lineberger, in *The Chemical Dynamics and Kinetics of Small Radicals*, edited by K. Liu and A. Wagner (World Scientific Publishing Co., Singapore, 1995), Vol. 6, p. 616.
[36] J. M. Papanikolas, J. R. Gord, N. E. Levinger, D. Ray, V. Vorsa, and W. C. Lineberger, J. Phys. Chem. **95**, 8028 (1991).
[37] D. Ray, N. E. Levinger, J. M. Papanikolas, and W. C. Lineberger, J. Chem. Phys. **91**, 6533 (1989).
[38] A. Sanov, S. Nandi, and W. C. Lineberger (unpublished).
[39] R. M. Bowman, M. Dantus, and A. H. Zewail, Chem. Phys. Lett. **161**, 297 (1989).
[40] M. Gruebele and A. H. Zewail, J. Chem. Phys. **98**, 883 (1993).
[41] E. D. Potter, J. L. Herek, S. Pedersen, Q. Liu, and A. H. Zewail, Nature (London) **355**, 66 (1992).
[42] M. Shapiro and P. Brumer, Int. Rev. Phys. Chem. **13**, 187 (1994).
[43] M. Shapiro and P. Brumer, J. Chem. Soc. Faraday Trans. **93**, 1263 (1997).
[44] A. H. Zewail, J. Phys. Chem. **100**, 12701 (1996).
[45] D. Tannor and S. A. Rice, Adv. Chem. Phys. **70**, 441 (1988).
[46] J. Faeder, N. Delaney, P. E. Maslen, and R. Parson, Chem. Phys. Lett. **270**, 196 (1997).
[47] M. T. Zanni, T. R. Taylor, B. J. Greenblatt, B. Soep, and D. M. Neumark, J. Chem. Phys. **107**, 7613 (1997).
[48] P. E. Maslen, J. M. Papanikolas, J. Faeder, R. Parson, and S. V. Oneil, J. Chem. Phys. **101**, 5731 (1994).
[49] M. E. Nadal, P. D. Kleiber, and W. C. Lineberger, J. Chem. Phys. **105**, 504 (1996).
[50] S. Nandi, A. Sanov, N. Delaney, R. Parson, and W. C. Lineberger (unpublished).
[51] J. W. Che, M. Messina, K. R. Wilson, V. A. Apkarian, Z. Li, C. C. Martens, R. Zadoyan, and Y. J. Yan, J. Phys. Chem. **100**, 7873 (1996).
[52] Z. D. Chen, M. Shapiro, and P. Bruner, Phys. Rev. A **52**, 2225 (1995).
[53] M. Blackwell, P. Ludowise, and Y. Chen, J. Chem. Phys. **107**, 283 (1997).
[54] C. J. Bardeen, V. V. Yakovlev, K. R. Wilson, S. D. Carpenter, P. M. Weber, and W. S. Warren, Chem. Phys. Lett. (in press).